# Experimental transition probabilities and Stark-broadening parameters of neutral and singly ionized tin

Myron H. Miller
*Institute for Physical Science and Technology, University of Maryland, College Park, Maryland 20742 and Department of Mechanical Engineering, United States Naval Academy, Annapolis, Maryland 21402*

Randy A. Roig*
*Institute for Physical Science and Technology, University of Maryland, College Park, Maryland 20742*

Roger D. Bengtson
*Department of Physics, University of Texas, Austin, Texas 78712*
(Received 15 December 1978)

Strengths and Stark-effect widths of the Sn I and Sn II lines prominent between 3200 and 7900 Å are measured with a spectroscopic shock tube. Absolute strengths of 17 ionic lines are obtained with estimated (22–50)% accuracy and conform to appropriate quantum-mechanical sum rules. Relative transition probabilities for nine prominent neutral tin lines, normalized to radiative-lifetime data, are compared with other experiments and theoretical predictions. Parameters for Stark-effect broadening are measured over a range of plasma electron densities. Broadening data [with accuracies of (15–35)%] for one neutral and ten ionic lines of tin are compared to theoretical predictions.

## INTRODUCTION

The atomic optical constants of heavy elements are the subject of increasing theoretical and experimental work.[1] Leading transitions in the visible spectrum of singly ionized tin involve a single optical electron whose energy levels are well separated. This simple structure allows relativistic[2] and ordinary[3] central field calculations of heavy emitter line strengths to be compared without undue error from computational complexity or configuration mixing. Additionally, one-electron (Wigner-Kirkwood and Thomas-Reiche-Kuhn) sum rules[4] can be used to assess experimental $gf$ values. The 17 Sn II line strengths reported here, some for the first time,[5,6] comprise several complete transition arrays, so that results can be further tested against the $J$-file sum rules.[7] Stark-effect broadening of these lines is marked, which reduces chances for self-absorption in measurement of $gf$ values and facilitates curve-of-growth analyses if these data are subsequently used for astrophysical investigations. The robust widths of these ionic lines lend themselves to a precise determination of Stark-broadening parameters, which for elements beyond the second period have heretofore been obtained quantitatively in only a few ions.[8,9]

Strengths of the brighter neutral tin lines (mainly in the uv) are measured as a complement to recent radiative-lifetime determinations.[10-14] Spectroscopic source conditions tailored to our Sn II investigations gave good signal-to-noise ratios for several Sn I lines. Shock-tube mean thermal energies are larger relative to interline differences in excitation potential than those common to previous studies of Sn I branching ratios.[15-18]

## EXPERIMENTAL

Apparatus and techniques for generating luminous plasmas, diagnosing thermodynamic conditions, and performing time-resolved emission spectroscopy are described in earlier papers.[19]

The spectral source was the luminous, essentially steady-state, plasma behind first- and multiple-reflected shock waves in a conventional shock tube. Prior testing of similar laminar ($6.7 \times 9.2$-cm$^2$ cross section) plasmas disclosed no repeatable inhomogeneities or departures from local thermodynamic equilibrium (LTE).[19] The test gas was 7–35 Torr of neon containing (0.2–0.4)% molal concentrations of tetramethyl tin, $Sn[CH_3]_4$. Shocks driven by 60–90 bars of ambient temperature hydrogen produced the experimental pressure-temperature domain shown in Fig. 1. The corresponding electron density range was $5-12 \times 10^{16}$ cm$^{-3}$. These source conditions were found to give optically thin profiles to both subject (Sn I, Sn II) and diagnostic ($H_\beta$, Ne I $\lambda = 5852$ Å) lines, provide good steady-state sampling times (30–200 $\mu$sec), and cover a broad range of photometric parameters (line-to-background ratio, absolute intensity, and line profile halfwidth) for purposes of regression analysis to test for experimental bias.

The 23 runs depicted in Fig. 1 were culled from a larger set on the basis of photometric quality,

 

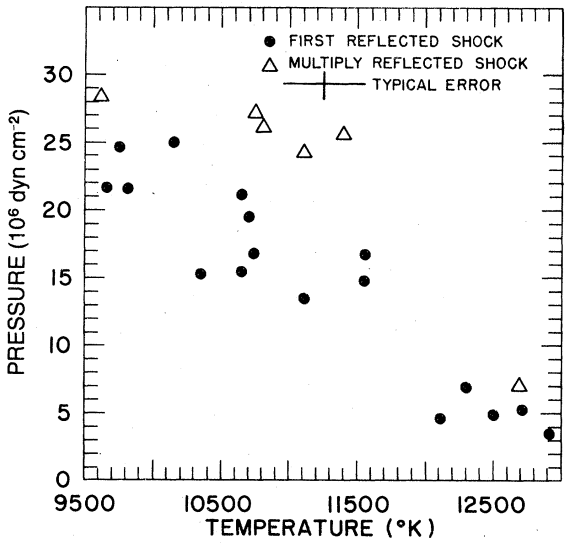


FIG. 1. Thermodynamic regime of the shock-tube experiments. Test gas initial composition is (0.2–0.4)% $Sn[CH_3]_4$ in research-grade neon.

completeness of thermodynamic data, and plasma steadiness during spectroscopic sampling times.

Plasma pressures were recorded by two piezoelectric transducers flush-mounted in the shock-tube walls. Temperatures were measured simultaneously three ways: by (photoelectrically) recording the absolute integrated intensities of $H_\beta$ and NeI $\lambda = 5852$ Å (excitation temperatures for upper levels at 12.7 and 18.6 eV, respectively), and by a reversal intensity determination[22] at 6562 Å (blackbody radiation temperature). Typical spreads between these redundant determinations, indicated in Fig. 1, were commensurate with estimated experimental errors and are similar to previous investigations using the same techniques.[19]

Profiles on tin lines were recorded photographically with a 1-m Fastie coma-corrected Czeny-Turner spectrograph ($f/8.6$). Resolution with fast emulsions (Kodak #2475, 103-0, 1-F) was 0.33–0.39 Å, depending on wavelength and film speed. Response characteristics of the emulsions were calibrated in the usual way with a well-regulated carbon arc and with a variety of transient sources.[19] Correction for radiative trapping was made by the computer code for converting specular densities to relative intensities: code input included absolute intensities photoelectrically recorded at several wavelengths and the optical depth measured at the core of $H_\alpha$ by the reversal intensity determination.[22] At the centers of the brightest tin lines (which by inspection could be seen to be much less bright than optically thick $H_\alpha$) this correction was seldom as large as 10%.

Organometallics such as $Sn[CH_3]_4$ are prone to decomposition in the presence of moisture. Precautions were taken to lessen chances for reaction of the tetramethyl tin with unspecified wall impurities during the several minutes test gases are in the tube prior to firing. The steel shock-tube and gas handling systems were cadmium plated to reduce porosity and moisture-trapping rust formation. A fresh batch of test gas was mixed each day. Preparatory evacuation of the system was to at least $10^{-6}$ Torr. An inductively driven spinner promoted mixing of the neon carrier and $Sn[CH_3]_4$ vapor.

It is estimated that tin losses exceeding a factor of 2 can be detected by comparison of plasma electron densities derived from $H_\beta$ halfwidths[20] with those, $[N_e(p,T)]$, computed from measured temperature, pressure, and initial gas composition.[21] A second method of inferring loss of $Sn[CH_3]_4$ is by comparing the absolute transition probabilities of SnI lines measured in emission (which depend directly upon plasma tin abundance) with $A$ values obtained from lifetime[10-14] data.

Both techniques indicated that the amount of tin in the spectroscopic plasmas was approximately one half that expected from initial mixture partial pressures.

An inadvertent, and imprecisely known, loss of tin affects shock-tube determinations of SnII and SnI absolute line strengths in distinctly different ways. Absolute SnII $A$ values are measured relative to the precisely known $A$ value (denoted $A_H$) of $H_\beta$.

$$A_{\mathrm{SnII}} = \frac{N_H}{N_{\mathrm{SnII}}} \frac{\lambda_{\mathrm{SnII}}}{\lambda_H} \frac{I_{\mathrm{SnII}}}{I_H} A_H , \tag{1}$$

where $I_{\mathrm{SnII}}/I_H$ is the measured ratio of energies in the subject and reference line integrated profiles and $N_H/N_{\mathrm{SnII}}$ is the corresponding population ratio. The SnII $\lambda = 5588$ Å/$H_\beta$ population ratio is not thermally sensitive, varying according to Fig. 2, by less than 30% throughout the 9600–12 400-K experimental range. The absolute abundance of tin affects the ratio only weakly through Saha equilibrium. Changing the abundance by a factor of $\frac{15}{6} = 2.5$ (corresponding to the experimental uncertainty in tin abundance) causes the population density ratio to shift less than 5%. These calculations are based on the assumption that a loss of $Sn[CH_3]_4$ results in the loss of all atomic species in $Sn[CH_3]_4$.

Transition probabilities for SnI lines were measured via

$$A_{\mathrm{SnI}} = I_{\mathrm{SnI}} 4\pi / hclN_{\mathrm{SnI}} , \tag{2}$$

where $l$ is the plasma thickness and $I_{\mathrm{Sn}}$ is the line's absolute integrated intensity. Because the ratio

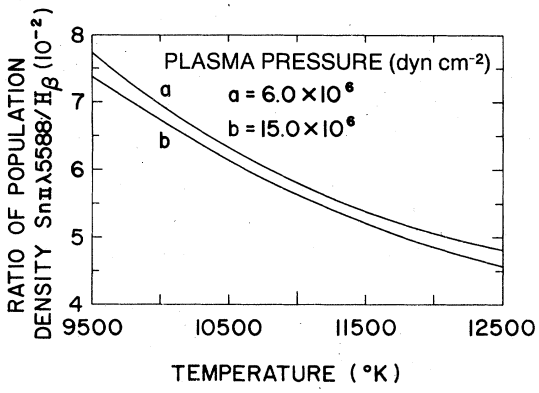


FIG. 2. Ratio of excited-state densities of Sn II $\lambda$ = 5588 Å-to-$H_\beta$ as a function of temperature for two plasma pressures. Test gas initial composition is 0.29% (molal) $Sn[CH_3]_4$ in neon. The population ratios at the two pressures (corresponding to a difference in plasma tin abundance of $\frac{15}{6}$ = 2.5) differ from one another less than 5% throughout the experimental domain.

of $N_{SnI}/N_H$ is critically sensitive to possible bias in temperature data, $H_\beta$ was not suitable as an "internal" standard. Figure 3 shows that an ambiguity in plasma tin abundance will carry over directly into the result. For this reason, absolute Sn I line strengths were used to estimate tin losses and relative Sn I line strengths were normalized using lifetime data.[10-14]

The partial widths of each tin line were measured at nine points (from 0.9 to 0.1 peak height) and fitted to an appropriate Voigt shape[23] as illustrated in Fig. 4(b). This technique allowed line wings to be readily discriminated from background. Precision in measuring the fitted profile area ratio of two tin lines (for determining relative $gf$ values) was typically (12–15)% per experiment for the

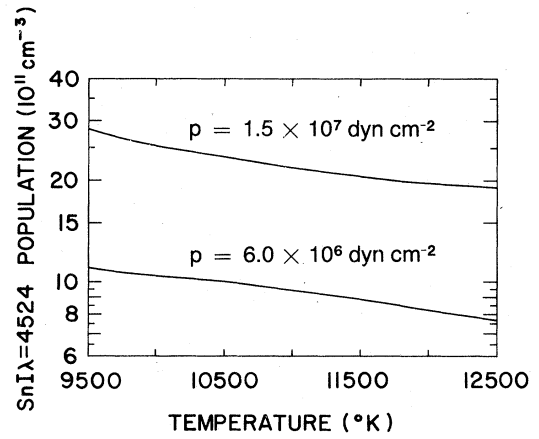


FIG. 3. Excited-state population density for Sn I $\lambda$ = 4524 Å vs temperature for two plasma pressures. Test gas initial composition is 0.25% $Sn[CH_3]_4$ in neon.

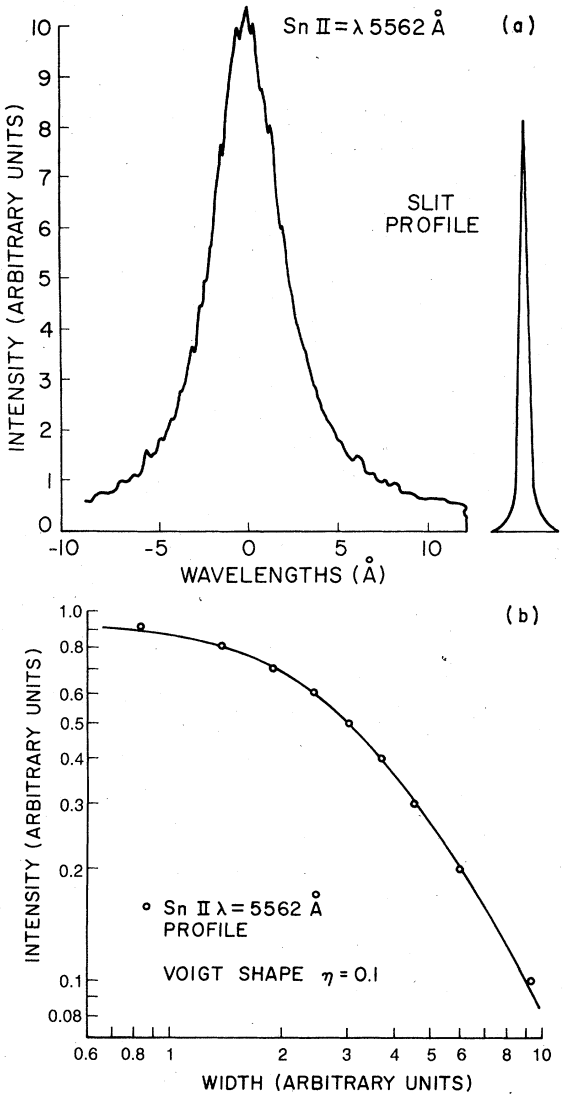


FIG. 4. (a) Intensity vs wavelength profile of Sn II $\lambda$ = 5562.0 Å recorded at a shock-tube electron density of $7.6 \times 10^{16}$ cm$^{-3}$. The instrumental profile (half-intensity width 0.38 Å) is shown for comparison. (b) Dimensionless comparison of the experimental Sn II $\lambda$ = 5562.0 Å profile (Fig. 4a) with the appropriate theoretical Voigt shape.

brighter profiles and approximately half of this for weaker lines. None of the fitted tin profiles showed indications of radiative trapping. Precision in relating the areas of a tin profile and $H_\beta$ [for determining absolute line strengths via Eq. (1)] was usually (15–20)% per experiment. The analogous precisions in obtaining the ratio of tin line and $H_\beta$ half intensity widths (where the latter is proportional to electron density to the 2/3 power) were generally (15–20)% per experiment. Because tin profiles were 3–15 times as broad as the instru-

mental profile, as illustrated in Fig. 4(a), deconvolution presented little likelihood of bias.[23,26] Plots of slit-corrected Lorentzian width components versus electron density were linear and extrapolated to zero intercepts within expected tolerances.

In some of the runs, the neutral carbon lines C I $\lambda = 5052$ Å and C I $\lambda = 5380$ Å attained useful brightness. Since the strengths[24,25] and broadening parameters[26-28] are known to 50% or better, the $gf$ values and Stark widths of these lines were measured in the same way as the tin lines to serve as an approximate control. In the case of both strengths and widths, present C I data were consistent with the literature.

## RESULTS AND DISCUSSION

Absolute transition probabilities for singly ionized tin are presented in Table I. Tolerances for shock-tube data represent a compounding of 90% confidence estimates of possible repeatable error with ($2\sigma$) observed random error. Stark broadening caused Sn II $\lambda = 5798.9$ Å to blend with Sn II $\lambda = 5796.9$ Å. Aside from this, there was no consequential blending or interference from impurity lines.

Ionic line strengths from the arc experiments of Wujec and Weniger[6] and Wujec and Musielok[5] come within mutual tolerance of shock-tube results for 10 out of the 12 lines measured in common.

TABLE I. Absolute transition probabilities ($10^8$ sec$^{-1}$) of Sn II.

| Multiplet [c] | $J_i$–$J_k$ | $E_i$–$E_k$ (cm$^{-1}$) | $\lambda$ (Å) | This work [a] | | Arc experiments: Wujec and Weniger [d] | Arc experiments: Wujec Musielok [e] | Theoretical predictions: CA-$LS$ [b] | Theoretical predictions: Migdalok [f] |
|---|---|---|---|---|---|---|---|---|---|
| $5s5p^2\,{}^4P$–$6p\,{}^2P^0$ | $2\frac{1}{2}$–$1\frac{1}{2}$ | 50730–72377 | 4618.3 | 0.0054 | *B* | ··· | ··· | ··· | ··· |
| $6s\,{}^2S$–$6p\,{}^2P^0$ | $\frac{1}{2}$–$1\frac{1}{2}$ | 56886–72377 | 6453.6 | 0.66 | *C* | 1.21 ±0.36 | ··· | 0.72 | 0.82 |
| | $\frac{1}{2}$–$\frac{1}{2}$ | 56886–71493 | 6844.2 | 0.61 | *B* | 0.66 ±0.21 | ··· | 0.60 | 0.70 |
| $5s5p^2\,{}^2D$–$6p\,{}^2P^0$ | $2\frac{1}{2}$–$1\frac{1}{2}$ | 59463–72377 | 7741.4 | 0.16 | *C* | ··· | ··· | ··· | ··· |
| | $1\frac{1}{2}$–$\frac{1}{2}$ | 58844–71493 | 7903.5 | 0.19 | *C* | ··· | ··· | ··· | ··· |
| $5s5p^2\,{}^2D$–$4f^2\,F^0$ | $2\frac{1}{2}$–$2\frac{1}{2}$ | 59463–89288 | 3352.0 | 0.61 | *C* | ··· | 1.0 ±0.2 | ··· | ··· |
| | $1\frac{1}{2}$–$2\frac{1}{2}$ | 58844–89294 | 3283.1 | 0.68 | *C* | ··· | 1.0 ±0.2 | ··· | ··· |
| $5d^2D$–$4f\,{}^2F^0$ | $2\frac{1}{2}$–$3\frac{1}{2}$ | 72048–89288 | 5798.9 | 0.74 | *B* | 0.81 ±0.29 | ··· | 1.72 | ··· |
| | $2\frac{1}{2}$–$2\frac{1}{2}$ | 72048–89294 | 5796.9 | 0.1 | *D* | 0.28 ±0.10 | ··· | 0.11 | ··· |
| | $1\frac{1}{2}$–$2\frac{1}{2}$ | 71406–89294 | 5588.8 | 1.10 | *A* | 0.87 ±0.35 | ··· | 1.72 | ··· |
| $6p\,{}^2P^0$–$7s\,{}^2S$ | $1\frac{1}{2}$–$\frac{1}{2}$ | 72377–86280 | 7190.8 | 0.71 | *C* | ··· | ··· | 0.65 | 0.75 |
| | $\frac{1}{2}$–$\frac{1}{2}$ | 71493–86280 | 6760.9 | 0.37 | *B* | 0.32 ±0.1 | ··· | 0.33 | 0.39 |
| $6p\,{}^2P^0$–$6d^2D$ | $1\frac{1}{2}$–$2\frac{1}{2}$ | 72377–90351 | 5562.0 | 1.30 | *A* | 1.18 ±0.40 | ··· | 0.87 | ··· |
| | $\frac{1}{2}$–$1\frac{1}{2}$ | 71493–90241 | 5332.4 | 1.20 | *A* | 0.86 ±0.31 | ··· | 0.74 | ··· |
| | $1\frac{1}{2}$–$1\frac{1}{2}$ | 72377–90241 | 5596.3 | 0.13 | *C* | 0.147 ±0.05 | ··· | 0.15 | ··· |
| $5d^2D$–$5f^2\,{}^2F^0$ | $2\frac{1}{2}$–$3\frac{1}{2}$ | 72048–99661 | 3620.5 | 0.020 | *D* | ··· | ··· | 0.081 | ··· |
| $6p\,{}^2P^0$–$7d^2D$ | $1\frac{1}{2}$–$2\frac{1}{2}$ | 72377–100330 | 3575.4 | 0.13 | *D* | ··· | 0.13 ±0.3 | 0.35 | ··· |
| | $\frac{1}{2}$–$1\frac{1}{2}$ | 71493–100284 | 3472.3 | 0.12 | *D* | ··· | 0.16 ±0.3 | 0.30 | ··· |

[a] Estimated uncertainty: $22\% < A \leq 28\%$, $25\% < B \leq 35\%$, $35\% < C \leq 50\%$, $D \geq 50\%$.
[b] Coulomb approximation (CA). Computed using tabulated integrals of radial wave functions (Ref. 3).
[c] Reference 29.
[d] Reference 6.
[e] Reference 5.
[f] Reference 2.

TABLE II. $J$-file sums for experimental Sn II line strengths.

| | | $6p$ | $^2P^0_{1/2}$ | $^2P^0_{3/2}$ |
|---|---|---|---|---|
| | $6s$ | | | |
| | $^2S_{1/2}$ | | 19.5 | 35.0 |
| File $\sum S/g$ | This work | | 9.8 | 8.8 |
| | Wujec | | 17.7 | 10.4 |

| | | $6p$ | $^2P^0_{1/2}$ | $^2P^0_{3/2}$ |
|---|---|---|---|---|
| | $7s$ | | | |
| | $^2S_{1/2}$ | | 11.8 | 26.0 |
| File $\sum S/g$ | This work | | 5.7 | 6.5 |

| | | $6d$ | $^2D_{3/2}$ | $^2D_{5/2}$ | File $\sum S/g$ This work | Wujec |
|---|---|---|---|---|---|---|
| | $6p$ | | | | | |
| | $^2P^0_{1/2}$ | | 40.0 | | 20.1 | 14.5 |
| | $^2P^0_{3/2}$ | | 4.5 | 66.2 | 17.7 | 16.3 |
| File $\sum S/g$ | This work | | 11.2 | 11.0 | | |
| | Wujec | | 8.5 | 10.1 | | |

| | | $5d$ | $^2D_{3/2}$ | $^2D_{5/2}$ | This work | Wujec |
|---|---|---|---|---|---|---|
| | $4f$ | | | | | |
| | $^2F^0_{5/2}$ | | 56.8 | 6.2 | 10.5 | 10.2 |
| | $^2F^0_{7/2}$ | | | 57.0 | 7.1 | 7.8 |
| File $\sum S/g$ | This work | | 14.2 | 10.5 | | |
| | Wujec | | 11.2 | 13.0 | | |

The largest disparity occurs for SnII $\lambda = 6453.6$ Å.

The column in Table I headed "CA-*LS*" contains scaled-central field (with *LS* coupling) approximations computed from tabulated integrals.[3] Migdalek[2] has calculated four transition probabilities shown in the adjacent column, taking exchange and relativistic effects into account. In this comparison, the simple and more refined theoretical predictions come equally close to experimental values.

Table II tests shock-tube and arc intramultiplet line strengths for conformity with the $J$-file sum rule.[7] File sums of shock-tube determined line strengths, when divided by file degeneracies, generally fluctuate little within a transition array.

Shock-tube $f$ values for ionized tin are arrayed in Table III to assess conformity with the Wigner-Kirkwood (WK) and Thomas-Reiche-Kuhn (TRK) sum rules.[4] The first two columns give multiplet oscillator strengths for allowed (one-electron) transitions to and from the $5s^2\,6p$ configuration. Experimental results have been augmented by Coulomb potential and asymptotic approximations,[3,4] which account for approximately $\frac{1}{3}$ of the column sums. According to the customary validity criteria,[30] these high $n$ computations should not cause serious uncertainty in the column sums. Alongside, the corresponding central field approximations are given as a test of computational accuracy. We have included the measurably strong two-electron $5s5p^2$-$5s^2\,6p$ transition in the sum. While this transition indicates that there is more than one optical electron, we feel that a comparison with the single-electron sum rule ($\sum f = 1$) is still of value in demonstrating the appropriate absolute scale for transition probabilities. The Wigner-Kirkwood[4] sum rules are valid for a one-electron system in a central potential in which the orbital angular momentum is a constant of the motion. It would be expected that we violate the assumptions of the Wigner-Kirkwood sum rules to a greater extent than the TRK sum rule. Indeed, we see a larger difference in comparisons with the WK sum rule than the TRK sum rule. We recognize the problems inherent in comparison of our data with a one-electron sum rule, but feel that the comparison of the sums over many transitions indicates an absence of gross errors in the absolute scale for transition probabilities.

Neutral tin line strengths measured in emission can be normalized to the lifetime data shown in Table IV. The mean of level crossing, Hanle, and beam-foil determinations provide an absolute $f$-value scale more accurately than could be obtained from the shock tube (even if no problems had been encountered with absolute tin abundance). The relative line strengths from the shock tube help to assess branching ratios needed to convert lifetimes to atomic optical constants and extend the lifetime-derived absolute scale to more highly excited arrays.

The shock-tube and comparison data for neutral tin given in Table V are normalized to a lifetime-derived $A$ value of $0.27 \times 10^8$ sec$^{-1}$ for SnI $\lambda = 3801.0$ Å. Lines with lower states near ground are prone to reabsorption in laminar boundary layers. Reabsorption dips in profiles could be readily detected in radiation from late multiple-reflected shocks having thick boundary layers. However, instrumental resolution is insufficient to disclose mild reabsorption as expected when boundary layers are still thin immediately behind shock waves.

TABLE III. Array average oscillator strengths for one-electron transitions involving $5s^2 6p$.

| Initial configuration | This work $6p$ | | Coulomb approximation $6p$ | |
|---|---|---|---|---|
| Final configurations | $ns$ | $nd$ | $ns$ | $nd$ |
| $n=5$ | −0.14 [a] | −0.02 [b] | ... | −0.02 |
| $n=6$ | −0.43 | 0.98 | −0.45 | 0.72 |
| $n=7$ | 0.26 | 0.06 | 0.24 | 0.10 |
| $n=8$ | 0.003 [c] | 0.056 [c] | 0.003 | 0.056 |
| $n=9-\infty$ | 0.005 [c] | 0.090 [c] | 0.005 | 0.090 |
| Continuum | 0.010 [d] | 0.206 [d] | 0.010 | 0.206 |
| Partial sum | −0.29 | 1.37 | −0.19 | 1.15 |
| WK sum-rule | ≅−0.11 | ≈1.11 | ≅−0.11 | ≅1.11 |
| Experimental sum | 1.08 | | 0.96 | |
| TRK sum rule | ≅1.00 | | ≅1.00 | |

[a] The multiplet averaged oscillator strength for $5s^2 6p\ ^2P^0$-$5s5p^2\ ^2D$ has been entered here.
[b] Computed using tabulated (Ref. 3) central field approximations and $LS$ coupling coefficients.
[c] Asymptotic approximations (Ref. 4).
[d] Bound-free contributions via scaled hydrogenic potentials (Ref. 4).

Tolerances have been adjusted for possible bias of (10–15)% on this account, and also incorporate (10–15)% error for the uncertainty in lifetime-cum-branching ratio data adopted for the Sn I $\lambda = 3801.0$ absolute $A$ value.

Theoretical calculations by Lawrence[31] and Warner[32] and several arc experiments furnish comparison values. Scatter between the relative line strengths obtained from various arcs is substantial and curious, in view of refinements to arc technique that occurred since to the pioneering work of Corliss.[15] Shock-tube results agree with the data of Penkin[16] and, if a single line is discounted from each comparison, agree also with results of Wujec,[16] Lotrian,[17] and Khoklov.[18] Predictions of Lawrence[31] approach our findings closely, while those of Warner[32] would be brought into agreement by scaling his relative result for Sn I $\lambda = 3801.0$ Å upwards by a factor of 2.

TABLE IV. Radiative lifetime data for the $5P6s\ ^3P_1^0$ state of Sn I.

| Method | author | $10^{-9}S$ |
|---|---|---|
| Phase shift | Lawrence [a] | 6.0 |
| Level crossing | Brieger *et al.* [b] | 4.5 |
| Hanle | deZafra *et al.* [c] | 4.84 |
| Hanle | Holmgren *et al.* [d] | 4.75 |
| Beam-foil | Anderson *et al.* [e] | 4.2 |

[a] Reference 10.
[b] Reference 11.
[c] Reference 12.
[d] Reference 13.
[e] Reference 14.

Stark-broadening parameters for the brighter isolated tin lines are given in Table VI. Data obtained over the range $5–12 \times 10^{16}$ cm$^{-3}$ are adjusted to an electron density of $10^{17}$ cm$^{-3}$. Random error (via analysis of variance) accounts for less than 50% of the stated estimated errors. Blending with the weak Sn II $\lambda = 5796.9$ Å line causes the uncertainty in the Sn II $\lambda = 5798.9$ Å width to be greater than that in the Sn II $\lambda = 5588.8$ Å line belonging to the same multiplet.

Electron impact widths computed by the semi-empirical formula[33] of Griem include broadening contributions from the three to four levels most strongly interacting with a line's upper and lower states. Quasistatic broadening by ions has been neglected. For most Sn II lines, theory and experiment agree within estimated experimental error; for the two out of seven comparisons where disagreement is larger, the disparity does not exceed the sum of the estimated experimental plus theoretical error.[9] The mean ratio of theoretical

TABLE V. Neutral tin transition probabilities, normalized to lifetime data.[a]

| Multiplet[d] | $J_i$–$J_k$ | λ (Å) | This work[b] | Absolute $A$ value, $10^8$ sec$^{-1}$ Corliss[e] | Penkin[f] | Wujec[g] | Lotrian[h] | Khoklov[i] | Lawrence[j] | Warner[k] |
|---|---|---|---|---|---|---|---|---|---|---|
| $5p^3P$–$6s\,^3P^0$ | 2–1 | 3175.0 | 0.98[c] *C* | 0.43 | 0.93 | 0.90 | 0.61 | 0.98 | 0.92 | 1.94 |
| $5p^1S$–$7s\,^3P^0$ | 0–1 | 3218.7 | 0.31 *C* | ··· | ··· | ··· | ··· | ··· | ··· | ··· |
| $5p^1D$–$6s\,^3P^0$ | 2–2 | 3330.6 | 0.20[c] *B* | 0.15 | 0.19 | 0.17 | 0.12 | 0.094 | 0.16 | 0.39 |
| $5p^1D$–$6s\,^3P^0$ | 2–1 | 3801.0 | 0.27[c] *REF* | 0.27 | 0.27 | 0.27 | 0.27 | 0.27 | 0.27 | 0.27 |
| $5p^1D$–$6s^1P^0$ | 2–1 | 3262.3 | 2.07[c] *C* | 1.48 | 3.02 | 1.90 | 2.45 | 2.46 | 3.02 | 4.38 |
| $5p^1D$–$5s5P^3\,^5S^0$ | 2–2 | 3223.6 | 0.02[c] *C* | ··· | ··· | 0.0012 | ··· | ··· | ··· | ··· |
| $5p^1S$–$6s\,^3P^0$ | 0–1 | 5631.7 | 0.18 *B* | 0.008 | ··· | ··· | ··· | ··· | 0.16 | 0.55 |
| $5p^1S$–$6s\,^1P^0$ | 0–1 | 4524.7 | 0.35 *B* | 0.19 | ··· | 0.26 | ··· | ··· | 0.25 | 0.76 |
| $5p^1S$–$7s\,^3P^0$ | 0–1 | 3655.8 | 0.16 *C* | 0.54 | ··· | 0.04 | 0.43 | ··· | ··· | ··· |

[a] Absolute $A$ value for 3801.0 determined from the lifetime data shown in Table V and the branching ratios of Penkin (Ref. 16).

[b] Estimated error: $35\% \leq B \leq 50\%$, $>50\% C$.

[c] Line core reabsorption (in laminar boundary layer) may reduce apparent line strength by as much as 20% without detection via distortion of profile shape.

[d] Reference 29.

[e] Reference 15.

[f] Reference 16.

[g] Reference 6.

[h] Reference 17.

[i] Reference 18.

[j] Reference 31.

[k] Reference 32.

TABLE VI. Stark-effect broadening of tin lines.

| Ion | Configuration (Ref. 29) | λ (Å) | Half-intensity width (Å) at $N_e = 10^{17}$ cm$^{-3}$ This work | Semiempirical theory[e] |
|---|---|---|---|---|
| Sn II | $6s\,^2S_{1/2}$–$6p\,^2P^0_{1/2}$ | 6844.2[d] | 4.2 ± 1.7[d] | 3.9 |
| | $6p\,^2P^0_{3/2}$–$6d\,^2D_{5/2}$ | 5562.0 | 5.1 ± 0.7 | 5.0 |
| | $6p\,^2P^0_{1/2}$–$6d\,^2D_{3/2}$ | 5332.4 | 5.3 ± 0.7 | 5.0 |
| | $5d\,^2D_{5/2}$–$4f^2F^0_{7/2}$ | 5798.9[c] | 4.2 ± 1.2[c] | 5.0 |
| | $5d\,^2D_{3/2}$–$4f^2F^0_{5/2}$ | 5588.8 | 3.8 ± 1.0 | 5.0 |
| | $6p\,^2P^0_{1/2}$–$7s\,^2S_{1/2}$ | 6760.9 | 5.5 ± 1.5 | 4.7 |
| | $6p\,^2P^0_{3/2}$–$7d\,^2D_{5/2}$ | 3575.4 | 3.0 ± 1.0 | 5.4 |
| | $5s5p^2\,^2D_{5/2}$–$4f^2F^0_{5/2}$ | 3352.0 | 2.5 ± 0.8 | ···[a] |
| | $5s5p^2\,^2D_{3/2}$–$4f^2F^0_{3/2}$ | 3283.1 | 2.3 ± 0.8 | ···[a] |
| | $5s5p^2\,^4P_{5/2}$–$6p\,^2P^0_{3/2}$ | 4816.3 | 1.6 ± 0.5 | ···[a] |
| Sn I | $5p^1S_0$–$6s\,^1P^0_1$ | 4524.7 | 1.3 ± 0.4 | ···[b] |

[a] Author's computations are for $LS$ coupling only.

[b] Theory not applicable.

[c] Blending reduces accuracy.

[d] Radiative trapping reduces accuracy.

[e] Reference 33.

to experimental widths is $1.14(\sigma/\sqrt{n} = 11\%)$, which is commensurate with findings from an extensive test of theory using experimental widths from ions in the first three atomic periods.[9]

ACKNOWLEDGMENT

This research was supported in part by NASA Grants No. NGR-21-002-007/8 and NSG-7347.

---

*Present address: Power Plant Siting Program, Tawes State Office Building, Annapolis, Md. 20742.

[1]J. R. Fuhr and W. L. Wiese, *Bibliography on Atomic Transition Probabilities*, U. S. Natl. Bur. Stand. Special Pub. 320, Suppl. 1 (U. S. GPO, Washington D. C., 1971), and subsequent private communication.

[2]J. Migdalek, J. Quant. Spectrosc. Radiat. Transfer 16, 265 (1976).

[3]G. Oertel and L. P. Shomo, Astrophys. J. Suppl. 16, 175 (1968).

[4]H. A. Bethe and E. E. Salpeter, *Quantum Mechanics of One-and-Two-Electron Atoms* (Springer, Berlin, 1957).

[5]T. Wujec and J. Musielok, Astron. Astrophys. 50, 405 (1976).

[6]T. Wujec and S. Weniger, J. Quant. Spectrosc. Radiat. Transfer 18, 509 (1977).

[7]E. U. Condon and G. H. Shortley, *The Theory of Atomic Spectra* (Cambridge, England, 1935).

[8]N. Konjevic and W. L. Wiese, J. Phys. Chem. Ref. Data 5, 259 (1976).

[9]W. W. Jones, Phys. Rev. A 7, 1826 (1973).

[10]G. M. Lawrence, J. K. King, and R. B. King, Astrophys. J. 141, 293 (1965).

[11]M. Brieger and P. Z. Zimmermann, Naturforschg. A 22, 2001 (1967).

[12]R. L. deZafra and A. Marshall, Phys. Rev. 170, 28 (1968).

[13]L. Holmgren and S. Svanberg, Phys. Scr. 5, 135 (1972).

[14]T. Anderson, O. H. Madsen, and G. Sorensen, J. Opt. Soc. Am. 62, 118 (1972).

[15]C. H. Corliss and W. R. Bozman, U.S. National Bureau Standard Monograph (U.S. GPO, Washington, D.C., 1962), Vol. 53.

[16]N. P. Penkin and I. Yu. Yu. Slavenas, Opt. Spectrosc. (USSR) 15, 83 (1963).

[17]J. Lotrian, J. Cariou, and A. Johannih-Gilles, J. Quant. Spectrosc. Radiat. Transfer 16, 315 (1976).

[18]M. Z. Khoklov, Izv. Krym. Astrofiz. Obs. 25, 249 (1961).

[19]M. H. Miller, R. A. Roig, and R. D. Bengtson, Phys. Rev. A 4, 1709 (1971); R. D. Bengtson, M. H. Miller, D. W. Koopman, and T. D. Wilkerson, *ibid.*, 3, 16 (1971); R. D. Bengtson, M. H. Miller, D. W. Koopman, and T. D. Wilkerson, Phys. Fluids 13, 372 (1970); M. H. Miller and R. D. Bengtson, Phys. Rev. A 1, 983 (1970).

[20]P. Kepple and H. R. Griem, Phys. Rev. 173, 317 (1968).

[21]H. R. Griem, Phys. Rev. 128, 997 (1962); D. W. Koopman, University of Maryland Tech. Note BN-481, 1966 (unpublished).

[22]M. H. Miller and R. D. Bengtson, J. Quant. Spectrosc. Radiat. Transfer 9, 1573 (1969).

[23]J. T. Davies and J. M. Vaughan, Astrophys. J. 137, 1302 (1963).

[24]W. L. Wiese, M. W. Smith, and B. M. Glennon, *Atomic Transition Probabilities*, U. S. Natl. Bur. Stand. Res. Ser. 4 (U. S. GPO, Washington, D. C., 1966).

[25]M. H. Miller, T. D. Wilkerson, R. A. Roig, and R. D. Bengtson, Phys. Rev. A 9, 2312 (1974).

[26]N. Konjevic and J. R. Roberts, J. Phys. Chem. Ref. Data 5, 209 (1976).

[27]M. H. Miller and R. D. Bengtson, Phys. Rev. A 1, 983 (1970).

[28]S. A. Freudenstein III, Stark Broadening in the Recombination Phase of a *Z*-Pinch Discharge, Ph.D. thesis (University of Colorado, 1977) (unpublished).

[29]W. G. Brill, Thesis (Purdue University, 1965) (unpublished).

[30]D. R. Bates and A. Damgaard, J. R. Astron. Soc. Lond. 242, 14 (1949).

[31]G. M. Lawrence, Astrophys. J. 148, 261 (1967).

[32]B. Warner and R. C. Kirkpatrick, Mon. Not. R. Astron. Soc. 142, 265 (1969).

[33]H. R. Griem, Phys. Rev. 165, 258 (1968).